World Academy of Science, Engineering and Technology
International Journal of Electronics and Communication Engineering
Vol:3, No:11, 2009

A Signal Driven Adaptive Resolution Short-Time Fourier Transform

Saeed Mian Qaisar, Laurent Fesquet and Marc Renaudin

***Abstract*—**The frequency contents of the non-stationary signals vary with time. For proper characterization of such signals, a smart time-frequency representation is necessary. Classically, the STFT (short-time Fourier transform) is employed for this purpose. Its limitation is the fixed time-frequency resolution. To overcome this drawback an enhanced STFT version is devised. It is based on the signal driven sampling scheme, which is named as the cross-level sampling. It can adapt the sampling frequency and the window function (length plus shape) by following the input signal local variations. This adaptation results into the proposed technique appealing features, which are the adaptive time-frequency resolution and the computational efficiency.

***Keywords*—**Level Crossing Sampling, Activity Selection, Adaptive Resolution Analysis, Computational Complexity.

I. Introduction

ALMOST all natural signals like speech, seismic and biological signals are of non stationary nature. Moreover the man made signals like Doppler, ASK (Amplitude Shift Keying), FSK (Frequency Shift Keying) etc. also lie in the same category. The spectral contents of these signals vary with time, which is a direct consequence of the signal generation process [5].

Classical systems are based on the Nyquist signal processing architectures. They cannot sense the input signal local variations and therefore they process it at a fixed pace. Thus, in case of low activity sporadic signals like electrocardiogram, phonocardiogram, seismic signals etc. they produce a large number of useless samples without any relevant information. It causes a useless increase in the system activity and so a useless increase of the power consumption.

Saeed Mian Qaisar has received his M.Sc degree in Electrical Engineering from INPG, France, in 2005. Currently he is a PhD candidate in Laboratory TIMA, CNRS UMR 5159, 46 Avenue Felix-Viallet, 38031 Grenoble Cedex, France (phone: +33-476574646; fax: +33-476574981; e-mail: saeed.mian-qaisar@imag.fr).

Laurent Fesquet is an associate professor at INPG and is working with Laboratory TIMA, CNRS UMR 5159, 46 Avenue Felix-Viallet, 38031 Grenoble Cedex, France (e-mail: laurent.fesquet@imag.fr).

Marc Renaudin was a professor at INPG, he is now with TIEMPO, the startup company he co-founded in July 2007, Tiempo SAS, 110 Rue Blaise Pascal, Bat Viseo – Inovallee, 38330 Montbonnot St Martin, France (e-mail: marc.renaudin@tiempo-ic.com).

The power efficiency can be achieved by smartly adapting the system computational load according to the input signal local variations. In this context, a signal driven sampling scheme, which is based on "level-crossing" is employed.

The LCSS (Level Crossing Sampling Scheme) [1] adapts the sampling rate by following the input signal local characteristics [12, 16]. Hence, it drastically reduces the post processing chain activity, because it only captures the relevant information [11, 13]. In this context, the LCSS based analog to digital converters have been developed [2, 4, 17]. Algorithms for processing [3, 11, 13, 18] and analysis [8, 12, 19] of the non-uniformly spaced out in time sampled data obtained with the LCSS have also been developed.

The focus of this work is to achieve a smart time-frequency representation of the time varying signals. The idea is to adapt the time-frequency resolution and the computational load according to the input signal local variations. It is realized by smartly combining the features of both uniform and non-uniform signal processing tools.

Section II briefly reviews the non-uniform signal processing tools employed in the proposed case. Complete functionality of the proposed technique is described in Section III. Its appealing features are further demonstrated with the help of a basic example in Section IV. Section V deals with the computational complexity and the processing error. In Section VI, the proposed technique performance is evaluated for a chirp signal. Section VII finally concludes the article.

II. Non-uniform Signal Processing Tools

A. LCSS (Level Crossing Sampling Scheme)

In recent years, there have been considerable interests in the LCSS, in a broad spectrum of technology and applications. In [20], authors have employed it for acquiring the non band limited signals. It has also been suggested in literature for random processes [21], band limited Gaussian random processes [22], compression [1] and for monitoring and control systems [23, 24, 25, 26]. The LCSS is also known as an event based sampling [27, 28].

In the case of LCSS, a sample is captured only when the input analog signal $x(t)$ crosses one of the predefined threshold levels [1]. The samples are not uniformly spaced in time because they depend on $x(t)$ variations as it is clear from Fig. 1. The non-uniformity in the sampling process reflects the signal local characteristics [12].

According to [1], the sampling instants of a non-uniformly sampled signal obtained with the LCSS are defined by Equation 1.

$$t_n = t_{n-1} + dt_n . \quad (1)$$

$$dt_n = t_n - t_{n-1} \quad (2)$$

Where t_n is the current sampling instant, t_{n-1} is the previous one and dt_n is the time delay between the current and the previous sampling instants (cf. Equation 2).

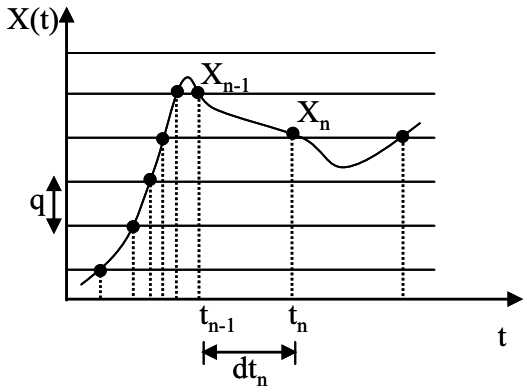

Fig. 1 Level crossing sampling scheme

B. LCADC (LCSS Based Analog to Digital Converter)

Classically, during an ideal A/D conversion process the sampling instants are exactly known, where as samples amplitudes are quantized at the ADC resolution [29]. This error is characterized by the SNR (Signal to Noise Ratio) [29]. Theoretically, the SNR of an ideal ADC can be calculated with Equation 3.

$$SNR_{dB} = 1.76 + 6.02.M \quad (3)$$

Where, M is the ADC number of bits, which defines its resolution. It shows that the SNR of an ideal ADC depends only upon M and it can be improved by 6.02 dB for each increment in M.

The A/D conversion process, which occurs in the LCADCs [2, 4, 17], is duel in nature. Ideally in this case samples amplitudes are exactly known, while the sampling instants are quantized at the timer resolution T_{timer}. According to [2, 4], the SNR in this case can be calculated by using Equation 4.

$$SNR_{dB} = 10.\log\left(\frac{3.P_x}{P_{x'}}\right) + 20.\log\left(\frac{1}{T_{timer}}\right) \quad (4)$$

Where, P_x and $P_{x'}$ are the powers of $x(t)$ and of its derivative respectively. It shows that in this case the SNR does not depend any more on M, but on $x(t)$ characteristics and T_{timer}. An improvement of 6.02 dB in the SNR can be achieved by simply halving T_{timer}.

Reconstruction issue of the non-uniformly sampled signal has been discussed in [27, 30, 31]. In [31], author showed that a bandlimited signal can be ideally reconstructed from its non-uniformly spaced samples, provided that the average number of samples satisfies the Nyquist criterion. In the case of LCADC, the number of samples is directly influenced by M and the signal characteristics [2, 4, 17]. Thus, for a given application an appropriate M should be chosen in order to respect the reconstruction criterion [21].

The LCADC advantages are discussed in [2, 4, 17]. The major among them are the reduced activity, the power saving, the reduced electromagnetic emission and the processing noise reduction. Inspiring from these features, the AADC (Asynchronous Analog to Digital Converter) [2] is employed to digitize $x(t)$ in the studied case. An M-bit AADC has $2^M - 1$ quantization levels which are disposed according to $x(t)$ amplitude range $\Delta x(t)$. In the case of AADC these levels are uniformly spaced. If ΔV_{in} is the AADC amplitude range then the AADC quantum q can be defined by Equation 5.

$$q = \frac{\Delta V_{in}}{2^M - 1} \quad (5)$$

Let δ be the AADC processing delay for one sample. Then for proper signal capturing, $x(t)$ must satisfy the tracking condition [2], given by Expression 6.

$$\frac{dx(t)}{dt} \le \frac{q}{\delta} \quad (6)$$

In order to respect the reconstruction criterion [31] and the tracking condition [2], a band pass filter with pass-band $[f_{min;}\, f_{max}]$ is employed at the AADC input. This together with a given M induces the AADC maximum and minimum sampling frequencies [11, 13], defined by Equations 7 and 8 respectively.

$$Fs_{\max} = 2.f_{\max}.(2^M - 1) \quad (7)$$

$$Fs_{\min} = 2.f_{\min}.(2^M - 1) \quad (8)$$

Where, f_{max} and f_{min} are the $x(t)$ bandwidth and fundamental frequencies respectively. Fs_{max} and Fs_{min} are the AADC maximum and minimum sampling frequencies respectively.

C. EASA (Enhanced Activity Selection Algorithm)

The EASA is an improved version of the ASA [8]. The relevant (active) parts of the non-uniformly sampled signal obtained with the AADC are selected by the EASA. This selection process corresponds to the adaptive length rectangular windowing process.

The main difference between the ASA and the EASA is the choice of the upper bound on the selected window length. For the ASA the time length in seconds and for the EASA the number of samples is chosen as the upper bound. The EASA

is defined as follow.

```
While (dtn ≤ T0/2 and Ni ≤ Nref)
        Ni = Ni + 1;
  end
```

Where, $T_0 = 1/f_{min}$ is the fundamental period of $x(t)$. T_0 and dt_n detect parts of the non-uniformly sampled signal with activity. This condition on dt_n is chosen in order to satisfy the Nyquist sampling criterion for f_{min}, when sampling $x(t)$ non-uniformly with the AADC. N^i represents the number of non-uniform samples lie in the i^{th} selected window W^i, which lie on the j^{th} active part of the non-uniformly sampled signal. Where, i and j both belong to the set of natural numbers $\mathbb{N}^*$. N_{ref} represents the upper bound on N^i. The choice of N_{ref} depends on the $x(t)$ characteristics and the system parameters.

The above described loop repeats for each selected window, which occurs during the observation length of $x(t)$. Every time before starting the next loop, i is incremented and N^i is initialized to zero.

For proper spectral representation, the condition given by Expression 9 should be satisfied [8]. Where, L^i is the length in seconds of W^i. In order to satisfy this condition for the worst case, which occurs for Fs_{max}, N_{ref} is calculated for an appropriate reference window length L_{ref}. L_{ref} has to satisfy the condition: $L_{ref} \geq T_0$. The process of calculating N_{ref} is given by Equation 10.

$$L^i \geq T_0 \tag{9}$$

$$N_{ref} = L_{ref}.Fs_{\max} \tag{10}$$

The lower and the upper bounds on L_{ref} are posed respectively by T_0 and the system resources (the maximum sample frame which system can process at once). For N_{ref} (cf. Equation 10), the condition 9 holds for all selected windows except for the case when the actual length of the j^{th} activity is less than T_0.

The EASA displays interesting features with the LCSS, which are not available in the classical case. It selects only the active parts of the non-uniformly sampled signal, obtained at the AADC output. Moreover, it correlates the length of the selected window with the input signal local characteristics.

III. Proposed Adaptive Resolution STFT

Block diagram of the proposed STFT is shown in Fig. 2. The activity selection and the local features extraction [8] are the proposed technique bases. They make to achieve the adaptive rate sampling and the adaptive resolution analysis. The approaches to realize it are detailed in the following subsections.

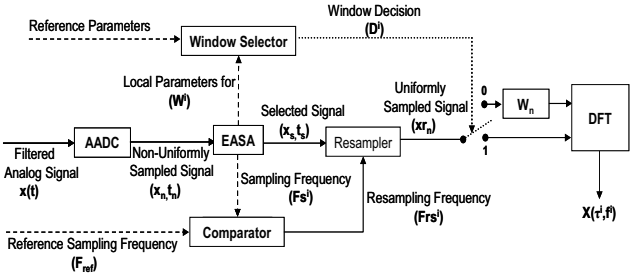

Fig. 2 Block diagram of the proposed STFT. '—' represents the signal flow, '···' represents the window shape decision flow and '----' represents the parameters flow at system different stages.

A. Adaptive Rate Sampling

The AADC sampling frequency is correlated to $x(t)$ local variations [8, 11]. Let Fs^i represents the AADC sampling frequency for W^i. Fs^i can be specific for each selected window, depending upon L^i and the slope of $x(t)$ part lying within this window [8]. It can be calculated by using the following equations.

$$L^i = t\max^i - t\min^i \tag{11}$$

$$Fs^i = \frac{N^i}{L^i} \tag{12}$$

In Equation 11, $tmax^i$ and $tmin^i$ are the final and the initial times of W^i. Please note that the upper and the lower bounds on Fs^i are posed by Fs_{max} and Fs_{min} respectively.

The sampled signal obtained at the AADC output can be used directly for further non-uniform digital processing [3, 12]. However in the studied case, the non-uniformity of the sampling process, which yields information on the signal local features, is employed to select only the relevant signal parts with the EASA. Furthermore the characteristics of each selected part are analyzed and are employed later on to adapt the proposed system parameters accordingly.

The selected signal is resampled uniformly before proceeding towards the further processing. The resampling frequency Frs^i of W^i is chosen depending upon the corresponding extracted features. Once the resampling is done, there are Nr^i samples in W^i. Choice of Frs^i is crucial and its selection procedure is detailed as follow.

In the proposed system a reference sampling frequency F_{ref} is chosen such as it remains greater than and closest to the $F_{Nyq}=2.f_{max}$. Depending upon values of F_{ref} and Fs^i, Frs^i can be chosen (cf. Fig. 2).

For the case, $Fs^i > F_{ref}$, Frs^i is chosen as: $Frs^i = F_{ref}$. It is done in order to resample the selected data, lies in W^i closer to the Nyquist frequency. It avoids the unnecessary interpolations during the data resampling process and so reduces the computational load of the proposed technique.

For the case, $Fs^i \leq F_{ref}$, Frs^i is chosen as: $Frs^i = Fs^i$. In this case, it appears that the data lie in the i^{th} selected window may be resampled at a frequency, which is less than the Nyquist frequency of $x(t)$ and so it can cause aliasing. Since, the

sampling rate of the AADC varies according to the slope of *x(t)* [2]. A high frequency signal part has a high slope and the AADC samples it at a higher rate and vice versa. Hence, a signal part with only low frequency components can be sampled by the AADC at a sub-Nyquist frequency of *x(t)*. But still this signal part is locally over-sampled in time with respect to its local bandwidth [11, 13, 18]. It is valid as far as $\Delta x(t) = \Delta V_{in}$, because it makes the relevant signal part to cross all thresholds of the AADC. This statement is further illustrated with the results summarized in Table II. Hence, there is no danger of aliasing, when the low frequency relevant signal parts are locally over-sampled in time at overall sub-Nyquist frequencies.

Due to the resampling process, there will be an additional error. Nevertheless, prior to this transformation, one can take advantage of the inherent over-sampling of the relevant signal parts in the system [11, 13, 18]. Hence, it adds to the accuracy of the post resampling process [4]. The NNRI (nearest neighbour resampling interpolation) is employed for data resampling. It is a simple interpolation method as it employs only one non-uniform observation for each resampled observation. Thus, it is efficient in terms of the computational complexity. Moreover, it provides an unbiased estimate of the original signal variance, due to this reason it is also known as a robust interpolation method [9, 10]. The detailed reasons of inclination towards NNRI are discussed in [8, 9, 10].

B. Adaptive Shape Windowing

The window selector implements the condition given by Expression 13. The output of window selector is the window decision D^i, which drives the switch state for W^i (c.f. Fig. 2).

$$if(N^i \le N_{ref} \quad and \quad (Td^i = t_1^i - t_{end}^{i-1}) > \frac{T_0}{2}) \tag{13}$$

In expression 13, t_1^i represents the 1^{st} sampling instant of the i^{th} selected window and t_{end}^{i-1} represents the last sampling instant of the $(i-1)^{th}$ selected window.

Jointly, the EASA and the window selector, provide an efficient spectral leakage reduction in the case of transient signals. Indeed, spectral leakage occurs due to the signal truncation problem, which causes to process the non integral number of cycles in the observation interval. Usually an appropriate smoothening (cosine) window function is employed to reduce the signal truncation, in the classical case. For the Please note that the references at the end of this proposed case, as long as the condition 13 is true, the leakage problem is resolved by avoiding the signal truncation [8]. As no signal truncation occurs so no cosine window is required. In this case, D^i is set to *1*, which drives the switch to state *1* in Fig. 2. Otherwise an appropriate cosine window is employed to reduce the signal truncation problem. In this case, D^i is set to *0*, which drives the switch to state *0* in Fig. 2.

C. Adaptive Resolution Analysis

The STFT is a classical tool, used for the time-frequency characterization of the time varying signals [6]. The STFT of a sampled signal x_n is determined by computing the DFT (Discrete Fourier Transform) of an N samples segment centred on τ, which describes the spectral contents of x_n around the instant τ. Where, N is defined by Equation 14.

$$N = L.Fs \tag{14}$$

In Equation 14, L is the effective length in seconds of the window function w_n and Fs is the sampling frequency. The STFT can be expressed mathematically by Equation 15.

$$X[\tau, f] = \sum_{n=\tau-\frac{L}{2}}^{\tau+\frac{L}{2}} [x_n . w_{n-\tau}] . e^{-j.2\pi.f.n} \tag{15}$$

In Equation 15, f is the frequency index, which is normalised with respect to F_s.

L controls the STFT time and frequency resolution [6]. In the classical case, the input signal is sampled at a fixed sampling frequency Fs, regardless of its local variations. Thus, a fixed L results into a fixed N (cf. Equation 14). In the case, when the spectrum of each windowed block is calculated with respect to τ and no overlapping is performed between the consecutive blocks, the time resolution Δt and the frequency resolution Δf of the STFT can be defined by Equations 16 and 17 respectively.

$$\Delta t = L \tag{16}$$

$$\Delta f = \frac{Fs}{N} \tag{17}$$

Equation 17 shows that for a fixed Fs, Δf can be increased by increasing N. But increasing N requires increasing L which will reduce Δt (cf. Equation 16). Thus, a larger L provides better Δf but poor Δt and vice versa. This conflict between Δf and Δt shows the limitation of the STFT, which is the reason for the creation of the MRA (multi resolution analysis) techniques [7, 14, 32]. The MRA techniques provide a good frequency but a poor time resolution for the low-frequency events and a good time but a poor frequency resolution for the high-frequency events. It is the type of analysis, best suited for most of the real life signals [7].

In this article, the fixed resolution dilemma is resolved to a certain extent by revising the STFT. The proposed STFT is a smart alternative of the MRA techniques. It performs adaptive time-frequency resolution analysis, which is not attainable with the classical STFT. It is achieved by adapting the Frs^i, L^i and Nr^i according to the local variations of *x(t)*. Thus, the time resolution Δt^i and the frequency resolution Δf^i of the proposed STFT can be specific for W^i and are defined by Equations 18

and 19 respectively.

$$\Delta t^i = L^i \tag{18}$$

$$\Delta f^i = \frac{Frs^i}{Nr^i} \tag{19}$$

Because of this adaptive time-frequency resolution, the proposed STFT will be named as the ARSTFT (adaptive resolution STFT), throughout the following parts of this article. This adaptive nature of the ARSTFT also leads towards a drastic computational gain, compared to the classical one. It is achieved firstly by avoiding the unnecessary samples to process and secondly by avoiding the use of the cosine window function as far as the condition 13 is true. The ARSTFT is defined by Equation 20.

$$X\left[\tau^i, f^i\right] = \sum_{n=\tau^i-\frac{Nr^i}{2}}^{\tau^i+\frac{Nr^i}{2}} \left[\{\mathrm{Re}\, sample(x_n, t_n)\}.w^i_{n-\tau^i}\right].e^{-j.2\pi.f^i.n} \tag{20}$$

Where, τ^i and f^i are the central time and the frequency index of the i^{th} selected window respectively. f^i is normalised with respect to Frs^i. n is the index of the resampled data points lie in W^i. The notation w_n^i represents that the window function length L^i and shape (rectangle or cosine) can be adapted for W^i.

IV. Basic Example

In order to illustrate the ARSTFT an input signal x(t), shown on the left part of Fig. 3 is employed. Its total duration is 30 seconds and it consists of four active parts. The summary of x(t) activities is given in Table I.

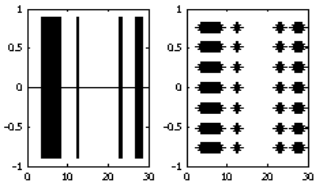

Fig. 3 Input signal (left) and the selected signal (right)

TABLE I
Summary of the Input Signal Activities

Activity	Signal Component	Length (Sec)
1st	0.9.sin(2.pi.50.t)	5
2nd	0.9.sin(2.pi.50.t)	0.4
3rd	0.9.sin(2.pi.200.t)	0.5
4th	0.9.sin(2.pi.500.t)	1.6

Table I shows that *x(t)* is band limited between 50 to 500 Hz. In this example *x(t)* is sampled by employing a 3-bit resolution AADC. Thus, Fs_{max} and Fs_{min} become 7 kHz and 0.7 kHz respectively (cf. Equations 7, 8). F_{ref} = 1.25 kHz is chosen, which satisfies the criteria given in Section II-C. ΔV_{in} = 1.8v is chosen, thus q becomes 0.2571v in this case (cf. Equation 5).

The selected signal obtained with the EASA is shown on the right part of Fig. 3. By following the criteria given in Section II-C, N_{ref} *=4096* is chosen, which leads to 6 selected windows. First three selected windows correspond to the first three activities and the remaining corresponds to the fourth activity. The last three selected windows are not distinguishable on the right part of Fig. 3, because they lie consecutively on the fourth activity. The parameters of each selected window are summarised in Table II.

TABLE II
Summary of the Selected Windows Parameters

Selected Window	L^i (Sec)	Fs^i (kHz)	N^i (Smp)	F_{REF} (kHz)	Frs^i (kHz)	Nr^i (Smp)
1st	4.99	0.7	3500	1.25	0.7	3500
2nd	0.39	0.7	280	1.25	0.7	280
3rd	0.49	2.8	1400	1.25	1.25	625
4th	0.58	7.0	4096	1.25	1.25	731
5th	0.58	7.0	4096	1.25	1.25	731
6th	0.43	7.0	3005	1.25	1.25	536

Table II exhibits the interesting features of the ARSTFT, which are achieved due to the smart combination of the non-uniform and the uniform signal processing tools. Fsi represents the sampling frequency adaptation by following the local variations of x(t). Ni shows that the relevant signal parts are locally oversampled in time with respect to their local bandwidths. Frsi shows the adaptation of the resampling frequency for Wi. It further adds to the ARSTFT computational gain, by avoiding the unnecessary interpolations during the resampling process. Nri shows that how the adjustment of Frsi avoids the processing of unnecessary samples during the spectral computation (cf. Equation 20). Li exhibits the EASA dynamic feature, which is to correlate the window function length with the local variations of x(t). Adaptation of Li, Frsi and Nri leads to the adaptive time-frequency resolution of the ARSTFT, which is clear from the values of Δti and Δf i in Table III.

TABLE III
The Selected Windows Time and Frequency Resolution

Window	1ST	2ND	3RD	4TH	5TH	6TH
Δt^i (Sec)	4.99	0.39	0.49	0.58	0.58	0.43
Δf^i (Hz)	0.2	2.5	2.0	1.71	1.71	2.33

Table III demonstrates that ARSTFT adapts its time-frequency resolution by following the local variations of x(t). It provides a good frequency but a poor time resolution for the low frequency parts of x(t) and vice versa. This type of analysis is best suited for most of the real life signals [7]. The spectrum of each selected window is computed and plotted with respect to τi on Fig. 4.

Fig. 4 shows the fundamental and the periodic spectrum peaks of each selected window. As Fs^1 and Fs^2 both remain less than F_{ref}, so $Frs^1 = Fs^1$ and $Frs^2 = Fs^2$ are chosen. Contrary, Fs^3 to Fs^6 all become greater than F_{ref}, thus Frs^3 to

Frs^6, all are chosen equal to F_{ref} (cf. Table II). The adaptation of Frs^i for W^i can be visualised on Fig. 4. In this case, for W^i the spectrum periodic frequency f_p^i is equal to Frs^i.

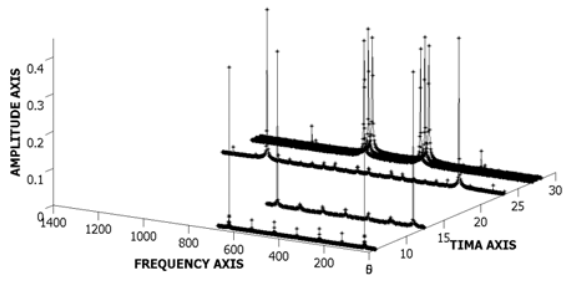

Fig. 4 The ARSTFT of the selected windows

The ARSTFT also adapts the window shape (rectangle or cosine), for W^i. The condition 13 remains true for the first three selected windows, thus D^i is set to 1. As no signal truncation occurs so no cosine window is required in this case. On the other hand, the number of samples for the fourth activity is 11200. Therefore, $N_{ref} = 4096$ leads to the three selected windows for the fourth activity time span. The condition 13 becomes false, thus D^i is set to *0*. As signal truncation occurs, so suitable length cosine (Hanning) windows are employed to reduce this effect.

In the classical case, if $Fs=F_{ref}$ is chosen, in order to satisfy the Nyquist sampling criterion for *x(t)*. Then the whole signal will be sampled at 1.25 kHz, regardless of its local variations. Moreover, the windowing process is not able to select only the active parts of the sampled signal. In addition, *L* remains static and is not able to adapt with *x(t)* local variations. This static nature makes the classical system to process unnecessary samples and so causes an increased computational activity than the proposed one. For this studied example, the fixed *N*=4096, will lead to nine fixed *L*=3.3 second windows, for the total *x(t)* time span of 30 seconds. It leads to the fixed $\Delta t=3.3$ seconds and $\Delta f=0.31$ Hz for all nine windows (cf. Equations 16 and 17).

V. Performance Evaluation

A. Computational Complexity

This section compares the computational complexity of the ARSTFT with the classical STFT. The complexity evaluation is made by considering the number of operations executed to perform the algorithm.

In the classical case, the sampling frequency and the window function length plus shape remains time invariant. If *N* is the number of samples lie in the window then the windowing operation will perform *N* multiplications between w_n and x_n (cf. Equation 15). The spectrum of the windowed data is obtained by computing its DFT. A complex term is involved in the DFT computation. The DFT complexity is calculated by taking the real and the imaginary parts separately. Thus, DFT performs *2N* multiplications and *2(N-1)* additions per output frequency. For larger values of *N*, $2.(N-1) \approx 2.N$. Thus, the DFT computational complexity for *N* output frequencies becomes $2.(N)^2$ additions and $2.(N)^2$ multiplications. The combine computational complexity C_1 of the STFT is given by Equation 21.

For the proposed ARSTFT, Fs^i, Frs^i and w_n^i are not fixed and are adapted for W^i, according to the local variations of *x(t)*. In comparison to the classical case, this approach locally requires some extra operations for each selected window. The EASA performs $2.N^i$ comparisons and N^i increments for W^i (cf. Section II-C). The choice of Frs^i and window shape, require three comparisons. The selected signal is resampled before computing its DFT. The NNRI is employed for the resampling purpose. The NNRI only requires a comparison operation for each resampled observation. Therefore, the resampler performs Nr^i comparisons. If $D^i = 0$, then a cosine window function is applied on the resampled data, which performs Nr^i multiplications (cf. Fig. 2). The DFT performs $2.(Nr^i)^2$ additions and $2.(Nr^i)^2$ multiplications for W^i. The combine computational complexity C_2 of the ARSTFT is given by Equation 22.

$$C_1 = A.\left[\underbrace{N + 2.(N)^2}_{Multiplications} + \underbrace{2.(N)^2}_{Additions}\right] \tag{21}$$

$$C_2 = \sum_{i=1}^{K} \underbrace{N^i}_{Increments} + \underbrace{2N^i + 3 + Nr^i}_{Comparisons} + \underbrace{\alpha Nr^i + 2(Nr^i)^2}_{Multiplications} + \underbrace{2(Nr^i)^2}_{Additions} \tag{22}$$

In Equation 21, A is the total number of windows, occurs for the observation length of x(t). In Equation 22, i=1,2,..,K represents the index of the selected window. α is a multiplying factor, its value is 1 if $D^i = 0$ and 0 if $D^i = 1$. From C_1 and C_2 it is clear that there are uncommon operations between both techniques. In order to make them approximately comparable the following assumption is made.

- *An increment or a comparison has the same processing cost as that of an addition.*

By following this assumption, comparisons and increments are merged into additions count, during the complexity evaluation process. The computational comparison of the ARSTFT with the classical one is made for results of the basic example. The gains are summarized in Table IV.

TABLE IV
SUMMARY OF THE COMPUTATIONAL GAIN

Time Span (Sec)	Gain in Additions	Gain in Multiplications
1st activity	2.737	2.739
2nd activity	212.473	214.021
3rd activity	42.686	42.955
4th activity	12.213	12.365

Table IV shows the gain in additions and multiplications of

the ARSTFT over the classical STFT for each *x(t)* activity. It demonstrates that the ARSTFT leads to a significant reduction of the total number of operations as compare to the classical STFT. This reduction in operations is achieved by adapting Fs^i, Frs^i and w_n^i according to the local variations of *x(t)*.

B. Resampling Error

In the proposed techniques the resampling is performed, which changes the properties of the resampled signal with respect to the original one. This error mainly contains of two effects. The time-amplitude pairs uncertainties which occur due to the AADC finite timer and threshold levels precision. The interpolation error which occurs during the uniform resampling process, considering their combine effect, the Mean resampling Error for W^i can be computed by employing the following Equation.

$$MRE^i = \frac{1}{Nr^i}.\sum_{n=1}^{Nr^i} \left| xo_n - xr_n \right| \tag{23}$$

Where, xr_n is the n^{th} resampled observation, interpolated with respect to the time instant tr_n. xo_n is the original sample value which should be obtained by sampling *x(t)* at tr_n. In the studied example discussed in Section IV, *x(t)* is analytically known, thus it is possible to compute its original samples values at any given time instant. It allows to compute the resampling error introduced by the proposed technique by employing Equation 23.

The mean interpolation error is calculated for each selected window. The results are summarized in Table V.

TABLE V
MEAN INTERPOLATION ERROR FOR EACH SELECTED WINDOW

Window	1st	2nd	3rd	4th	5th	6th
MIe^i(dB)	-26.3	-26.2	-25.9	-24.1	-24.1	-23.8

Table V shows that the error introduced by the resampling process is quite a minor one. In the case of high precision applications, the resampling error can be further reduced by increasing the AADC resolution *M* and the interpolation order [4, 11, 15]. Thus, an increased accuracy can be achieved at the cost of an increased computational load. Therefore, by making a suitable compromise between the accuracy level and the computational load, an appropriate solution can be devised for a given application.

VI. CASE STUDY

The instantaneous frequency of a chirp signal varies with time. The chirp-like signals are common in real life applications, like sonar and radar systems, spread spectrum communications, acoustic sounds etc. Being a common example of various time varying systems, it is employed to study the proposed technique performance.

The input chirp signal *x(t)* is bandlimited between 10 Hz to 500 Hz and its total duration is 8 sec. In the first quarter of time span, its frequency rises from 10 Hz to 500 Hz and contrary in the second quarter, it falls from 500 Hz to 10 Hz. The same pattern is repeated onwards. *x(t)* frequency pattern can be visualized from Fig. 5.

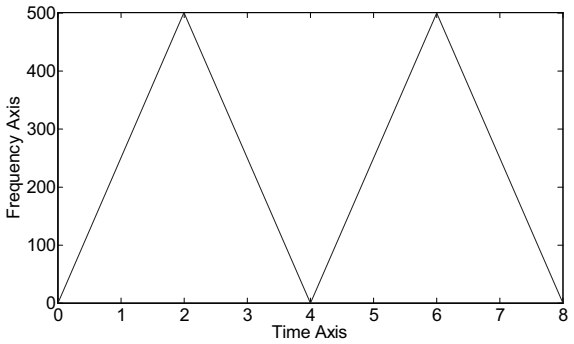

Fig. 5 The input signal frequency pattern

A 3-bit resolution AADC is used for digitizing *x(t)*and therefore, we have Fs_{min}= 140 Hz and Fs_{max}= 7000 Hz. The amplitude range is always set to ΔV_{in}=1.8 V, which leads to a quantum q = 0.257 V. The amplitude of *x(t)* is normalized to 0.9 V in order to avoid the AADC saturation.

With the given specifications, 10858 samples are obtained at the AADC output. In order to apply EASA, N_{ref} *=1024* is chosen, which satisfies the criteria given in Section II-C. For the chosen N_{ref}, EASA delivers 11 selected windows. The selected windows parameters are summarized in Table VI.

TABLE VI
SUMMARY OF THE SELECTED WINDOWS PARAMETERS

Selected Window	L^i (Sec)	Fs^i (kHz)	N^i (Smp)	F_{ref} (kHz)	Frs^i (kHz)	Nr^i (Smp)
1st	0.93	1099	1024	1250	1099	1024
2nd	0.32	3206	1024	1250	1250	400
3rd	0.24	4177	1024	1250	1250	300
4th	0.20	4945	1024	1250	1250	250
5th	0.18	5629	1024	1250	1250	225
6th	0.16	6205	1024	1250	1250	200
7th	0.15	6575	1024	1250	1250	187
8th	0.31	3294	1024	1250	1250	387
9th	0.38	2697	1024	1250	1250	475
10th	0.53	1910	1024	1250	1250	662
11th	0.77	797	618	1250	797	618

The time-frequency resolution values for the ARSTFT are calculated by employing Equations 18 and 19. The results are summarized in Table VII.

Tables VI and VII combinely demonstrate the ARSTFT signal driven nature. They show the adaptation of its sampling frequency and time-frequency resolution by following the input signal local variations. Contrary in the classical STFT, the sampling frequency and the window function remain time invariant. If the sampling is performed at F_{ref} = 1250 Hz, then for the 1024 samples 10 windows will be obtained, among them each one will be of 0.82 sec length. It will lead towards its fixed Δt = 0.82 sec and Δf = 1.2 Hz values (cf. Equations 16 and 17).

TABLE VII
THE SELECTED WINDOWS TIME AND FREQUENCY RESOLUTION

Selected Window	Δt^i (Sec)	Δf^i (Hz)
1st	0.93	1.1
2nd	0.32	3.1
3rd	0.24	4.2
4th	0.20	5.0
5th	0.18	5.5
6th	0.16	6.3
7th	0.15	6.6
8th	0.31	3.3
9th	0.38	2.6
10th	0.53	1.8
11th	0.77	1.0

The resampling error is calculated by employing Equation 23, which is bounded by -23.8 dB for all selected windows. It shows the proposed system accuracy. Further resampling accuracy can be achieved by increasing the AADC resolution and the interpolation order [4, 11, 15].

The computational gain of the ARSTFT over the classical one is also calculated by employing Equations 21 and 22. It shows 3.8 and 3.9 times gains in additions and multiplications respectively. It confirms the out performance of the ARSTFT over the classical one, even in the case of a continuously varying chirp signal. It is achieved due to the joint benefits of the AADC, the ASA and the resampling, as they make to adapt the sampling frequency and the window function (length plus shape) according to the signal local characteristics.

VII. CONCLUSION

A new tool for the adaptive resolution time-frequency analysis has been proposed. The ARSTFT is especially well suited for the low activity sporadic signals. It is shown that Fsi and Li change by following the x(t) local variations. Criteria to choose the appropriate Fref and Nref are developed. A complete methodology of choosing Frsi and wni for the ith selected window has been demonstrated. It is shown that the ARSTFT adapts its time-frequency resolution by following the local variations of x(t).

The resampling error is calculated. It is shown that the errors made for the studied cases are minor ones. Moreover, a higher accuracy can be achieved by increasing the AADC resolution and the interpolation order. Thus, an accuracy improvement can be achieved at the cost of an increased computational load.

The ARSTFT outperforms the STFT. The first advantage of the ARSTFT over the STFT is the adaptive time-frequency resolution and the second one is the computational gain. These smart features of the ARSTFT are achieved due to the joint benefits of the AADC, the EASA and the resampling, as they enable to adapt Fs^i, Frs^i, N^i, Nr^i and w_n^i by exploiting the local variations of $x(t)$.

The employment of fast algorithms in place of the DFT for the spectrum computation is in progress. It will add up to the computational gain of the ARSTFT.

The ARSTFT application for the real life signals is a prospect. Moreover, performance comparison of the ARSTFT with the MRA techniques in terms of computational complexity and quality is an area of future research.

REFERENCES

[1] J.W. Mark and T.D. Todd, "A nonuniform sampling approach to data compression", IEEE Transactions on Communications, vol. COM-29, pp. 24-32, January 1981.
[2] E. Allier, G. Sicard, L. Fesquet and M. Renaudin, "A new class of asynchronous A/D converters based on time quantization", ASYNC'03, pp.197-205, May 2003.
[3] F. Aeschlimann, E. Allier, L. Fesquet and M. Renaudin, "Asynchronus FIR filters, towards a new digital processing chain", ASYNC'04, pp. 198-206, April 2004.
[4] N. Sayiner, H.V. Sorensen and T.R. Viswanathan, "A Level-Crossing Sampling Scheme for A/D Conversion", IEEE Transactions on Circuits and Systems II, vol. 43, pp. 335-339, April 1996.
[5] S.C. Sekhar and T.V. Sreenivas, "Adaptive window zero-crossing based instantaneous frequency estimation", EURASIP Journal on Applied Signal Processing, pp.1791-1806, Issue 1, January 2004.
[6] D. Gabor, "Theory of communication", Journal of the IEE, Vol.93(3), pp.429-457, 1946.
[7] R. Polikar, "The engineer's ultimate guide to wavelet analysis", Rowan University, College of Engineering, retrieved June, 2006.
[8] S. M. Qaisar, L. Fesquet and M. Renaudin, "Spectral Analysis of a signal Driven Sampling Scheme", EUSIPCO'06, September 2006.
[9] S. de Waele and P.M.T.Broersen, "Time domain error measures for resampled irregular data", IEEE Transactions on Instrumentation and Measurements, pp.751-756, May 1999.
[10] S. de Waele and P.M.T.Broersen, "Error measures for resampled irregular data", IEEE Transactions on Instrumentation and Measurements, pp.216-222, April 2000.
[11] S. M. Qaisar, L. Fesquet and M. Renaudin, "Computationally efficient adaptive rate sampling and filtering", EUSIPCO'07, pp.2139-2143, September 2007.
[12] M. Gretains, "Time-frequency representation based chirp like signal analysis using multiple level crossings", EUSIPCO'07, pp.2154-2158, Sep-tember 2007.
[13] S. M. Qaisar, L. Fesquet and M. Renaudin, "Adaptive rate filtering for a signal driven sampling scheme", ICASSP'07, pp.1465-1468, April 2007.
[14] M. Vetterli et al. "Wavelets and filter banks: Theory and design", IEEE Transections on signal processing, Vol.40, pp.2207-2232, 1992.
[15] F. Harris, "Multirate signal processing in communication systems", EUSIPCO'07, September 2007.
[16] K. M. Guan and A.C. Singer, "Oppertunistic Sampling by Level-Crossing", ICASSP'07, pp.1513-1516, April 2007.
[17] F. Akopyan, R. Manohar and A.B. Apsel, "A level-crossing flash analog-to-digital converter", ASYNC'06, pp.12-22, Grenoble, France, March 2006.
[18] S.M. Qaisar, L. Fesquet and M. Renaudin, "Computationally efficient adaptive rate sampling and filtering for low power embedded systems", SampTA'07, June 2007.
[19] S.M. Qaisar, L. Fesquet and M. Renaudin, "An Adaptive resolution computationally efficient short time Fourier transform", EURASIP, Research Letters in Signal Processing, April 2008.
[20] K. Guan and A.C. Singer, "A level crossing sampling scheme for non-bandlimited signals", ICASSP'06, pp. 381-383, May 2006.
[21] I.F Blake and W.C. Lindsey, "Level-Crossing problems for random processes", IEEE transactions on information theory, pp. 295-315, 1973.
[22] M. Miskowicz, "Efficiency of level-crossing sampling for bandlimited Gaussian random process", Proc. of IEEE international workshop on factory communication systems-2006, pp. 137-142, June 2006.
[23] K.J. Astrom, B. Bernhardsson, "Comparison of periodic and event based sampling for first-order stochastic systems", Proc. of IFAC World Congress-1999, pp. 301-306, 1999.
[24] M. Miskowicz, "Send-on-delta concept: an event-based data reporting strategy", Sensors, vol 6, pp. 49-63, 2006.
[25] P. Otanez, J. Moyne and D. Tilbury, "Using deadbands to reduce communication in networked control systems", Proc. of American control conference'02, pp. 3015-3020, 2002.

[26] S.C. Gupta, "Increasing the sampling efficiency for a control system", IEEE transactions on automatic and control, pp. 263-264, 1963.
[27] M. Lim, C. Saloma, "Direct signal recovery from threshold crossings", Phys. Rev. E 58, pp. 6759-6765, 1998.
[28] M. Miskowicz, "Asymptotic effectiveness of the event-based sampling according to the integral criterion", Sensors, vol 7, pp. 16-37, 2007.
[29] R.H. Walden, "Analog-to-Digital converter survey and analysis", IEEE journal on selected areas in communications, vol. 17, pp. 539-550, April 1999.
[30] F.J. Beutler, "Error free recovery from irregularly spaced samples", SIAM Review, vol. 8, pp. 328-335, 1996.
[31] F. Marvasti, "Nonuniform sampling theory and practice", Kluwer academic/Plenum Publisher, New York, 2001.
[32] Ingrid Daubechies "Ten lectures on wavelets", Society for Industrial and Applied Mathematics, U.S, June 1992.